

See discussions, stats, and author profiles for this publication at: <https://www.researchgate.net/publication/291346691>

Multimodal Analog Front-end for Wearable Bio- sensors

Conference Paper · November 2015

DOI: 10.1109/ICSENS.2015.7370501

CITATIONS

2

READS

484

4 authors, including:



Insoo Kim

UConn Health Center

49 PUBLICATIONS 405 CITATIONS

[SEE PROFILE](#)



Ryan Lobo

Uhnder

6 PUBLICATIONS 65 CITATIONS

[SEE PROFILE](#)



Yusuf Bhagat

Jabil Circuit

45 PUBLICATIONS 856 CITATIONS

[SEE PROFILE](#)

Some of the authors of this publication are also working on these related projects:



Flash ADC [View project](#)



DBNS FIR Filter [View project](#)

Multimodal Analog Front-end for Wearable Biosensors

Insoo Kim, Ryan Lobo, Johnny Homer and Yusuf A. Bhagat

Samsung Research America - Dallas

Richardson, Texas, USA

{insoo3.kim, ryan.loblo, j.homer, y.bhagat}@samsung.com

Abstract—Wearable sensors afford convenience in daily health monitoring, though many challenges in the development of such systems need to be overcome. Here, we present a low power, multimodal analog front-end (AFE) for wearable health monitoring sensors. The AFE integrated circuit was designed and fabricated with standard 65 nm CMOS technology. Three sensor AFEs, bio-potential, photoplethysmography (PPG) and bioelectrical impedance analysis (BIA), were integrated on the same die with an area of $2.5 \times 2.5 \text{ mm}^2$. The power consumption is within $380 \text{ } \mu\text{W}$ for single AFE operation modes and 1.92 mW for concurrent operation modes with a 1.2V power supply. Results from each individual AFE showed high-quality, motion-robust signals (Electrocardiogram, PPG and BIA) that correlated with those obtained from clinical grade gold-standard devices for similar applications. Such multi-functional, non-intrusive systems permit users to effortlessly self-monitor multiple physiological parameters.

Keywords—Analog Front-end, multimodal sensing, ECG, BIA, PPG, Wearable sensors

I. INTRODUCTION

Of late, both, the academic and industrial sectors have devoted considerable efforts in promoting wearable health monitoring technology by means of research and the development of wearable products from routine wellness to clinical applications. The rapid pace of innovation in this domain can be attributed to recent technological advances in miniature sensors, low-power integrated circuits and wireless communications that have enabled concurrent monitoring of heart rate, electrocardiogram (ECG), oxygen saturation, respiration rate, body temperature, blood pressure, Galvanic skin response (GSR), electroencephalogram (EEG) and blood glucose [1-3].

Meanwhile, the demand for measuring reliable physiological signals across the breadth of daily living activities including intense fitness training keeps increasing. Such measurements are seamlessly possible on the basis of higher front-end dynamic ranges and integration of data processing and artifact removal algorithms. Currently, each state-of-the-art bio-sensor produces at least 16-bit digital stream data with a maximum sampling rate between 250-1000 Hz. Hence the mobile host should be capable of processing data from multiple sensors.

This approach still requires overcoming several major challenges. For example, it needs breakthroughs in sensor hardware such as on-sensor signal processing to reduce data

transfer rates and computational burden of the mobile host. Current sensors are larger in size and consume more battery power than is optimal. Given these conditions, one has to balance trade-offs between user comfort, long-term wearability and reliable data communications. Further, most individuals may not want to wear such large sensors unless continuous monitoring of one or more health conditions is required.

Based on these factors, we believe the ideal solution for wearable health monitoring systems is to integrate as many functions and sensing modalities as possible into one small form-factor device for minimizing non-intrusiveness and maximizing user comfort. Along these lines, the most non-intrusive body location for a small wearable sensor system would be the wrist, particularly if the device can be fashioned as a watch. Nonetheless, a wrist-based sensor system would have to contend with challenges such as size limitations and the occurrence of motion artifacts. For example, a parameter like oxygen saturation can be measured at the ear, forehead, finger or wrist, but the probability of motion degradation of such measurements at the ear or forehead is relatively lower compared to motion occurrence at extremities like the wrist or fingers.

Faced with the aforementioned power consumption and size constraints, current state-of-the-art wrist-worn devices support either photoplethysmography (PPG) or ECG sensing with an accelerometer [3, 4]. Consumers can monitor their sleep efficiency and/or caloric expenditure by measuring heart rate and activity levels [3] with such devices. In principle, self-monitoring of several health parameters is feasible by integrating PPG, ECG, and bio-impedance analyzers (BIA) into the system. For example, blood pressure can be measured on the basis of PPG and ECG [5, 6] sensing or by virtue of Bio-impedance and ECG sensing concurrently [7].

Here, we report a novel analog front-end (AFE) IC that supports bio-potential measurement, bioelectrical impedance analysis (BIA), GSR and photoplethysmography (PPG) sensors. By sharing common components and employing multi-functional circuit design techniques, we were able to integrate several high-performance sensor AFEs, and consequently, achieve significant reductions in power consumption and physical area of the system.

II. MULTIMODAL SENSOR AFE DESIGN

The basic concept of the proposed AFE IC is to share common circuit components between each analog front-end

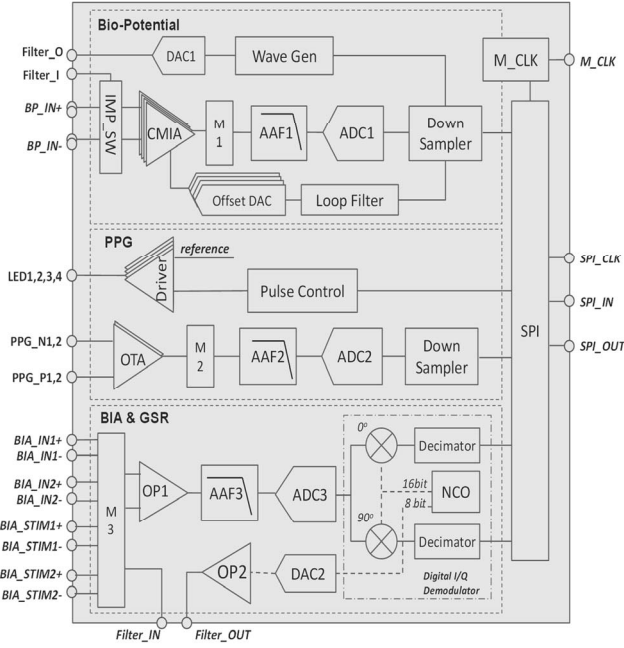


Fig. 1. Simplified schematic diagram of the multimodal sensor AFE IC.

dedicated for each sensing modality. In this design, the three frequently used sensor AFEs (Bio-potential, PPG and BIA AFEs) are integrated on the same die and shared output ports and logic controls (SPI, Serial Peripheral Interface) to substantially reduce power consumption and die size as shown in Fig. 1. Notably, the bio-potential and BIA AFEs may be merged since both AFEs have several components that are shared such as anti-aliasing filters (AAFs) and analog-to-digital converters (ADCs). However, the AFEs are separated in our implementation to further enhance the performance of each front-end by optimizing the circuit functionality in the analog signal pass. As shown in Fig. 1, BIA requires 8-to-4 full multiplexers (M3) at the inputs of OP1, whereas the analog multiplexer, M1, in the Bio-potential AFE should be placed between the CMIA and AAF1. Furthermore, the signal bandwidth of the BIA AFE ranges up to 1 MHz whereas that of the bio-potential AFE is maximally set to 500 Hz. Accordingly, the bandwidths of the AAF1 and AAF3 are set to 500 Hz and 1.2 MHz, respectively.

TABLE I
SUMMARY OF THE SYSTEM SPECIFICATIONS

Items	Bio-potential	PPG	BIA
Power Supply	1.2V	1.2V	1.2V
Number of Channels	4	2	2
Front-end Gain	42 dB	52 dB	7 dB
Signal Bandwidth	500 Hz	20 kHz	1 MHz
ADC Dynamic Range	60~94dB	60~94dB	60~94dB
Output Data Rate	8 kB/s	32 kB/s	3.84 kB/s
Main Feature	DC Offset Rejection	Auto gain Control Capability	Digital I/Q demodulator

Table 1 presents the summary of the design specifications of the AFE. The AFE takes a 1.2V single power supply to minimize the voltage overhead and to support low voltage battery operation. The Bio-potential AFE supports 4 channels of simultaneous signal acquisition with impedance monitoring and DC offset rejection features. The PPG AFE supports 4 LED drivers and 2 photodetectors, so that one can use two PPG sensors at the same time. The BIA AFE supports two differential input channels and two differential stimulation channels to facilitate both, segmental and whole body impedance measurements without having to reconfigure the measurement electrodes.

A. Bio-potential AFE

Unlike conventional instrumentation amplifiers (IAs), the common mode voltage of the IAs in the proposed design can be adjusted by the Offset DAC to reject input DC offsets which are created at the electrode-skin interface. The operation and results of the IA design was introduced elsewhere [8]. The IAs share AAF1 and ADC1 to increase the power and area efficiency. The AAF1 is designed with a 3rd order Sallen-Key low-pass filter. The cut-off frequency of the AAF1 is set to 500 Hz to account for the bandwidth of bio-potential signals such as ECG, EEG and EMG (electromyogram).

The ADC1 adapted the successive approximation register (SAR) architecture, which is known for low power consumption, and configured with 10 native digital bits. The sampling rate of the ADC1 can be set from 1 to 10 MHz depending on the master clock frequency, f_M , which can also be varied from 24-240 MHz based on desired applications. Relative to the signal bandwidth of 500 Hz, the sampling rate of the ADC1 is 1000 ~ 2500 times higher than the Nyquist sampling rate. By taking advantage of oversampling, we are able to increase the signal-to-noise ratio (SNR) of ADC1 by approximately 34 dB according to equation (1).

$$\text{SNR (dB)} = (6.02 \times N) + 1.76 + 10 \times \log (\text{OSR}) \quad (1)$$

where, N is the number of bits and the OSR is the oversampling rate. The Down Sampler in Fig. 1 averages the digitized data by the oversampling rate following which it increases the effective number of bits by 5-5.5.

B. PPG AFE

Although conventionally, PPG AFEs consist of only two LED drivers and one sensing channel, the current sensing AFE in our design is capable of driving four LEDs and receiving data from two photo-detectors for PPG sensing. Thus, two PPG sensors can be used at the same time through this AFE IC for applications that require multiple PPG sensors such as cuffless blood pressure monitoring [9].

The operational trans-conductance amplifier (OTA) is designed with the typical trans-impedance amplifier with a negative current feedback configuration. The OTA has preset gains from 40-100 dB with a 3 dB step to enable users to change the gain during acquisition. Furthermore, one can configure auto-gain control circuit by incorporating an algorithm to find the peak energy or amplitude of the acquired signals in an external microcontroller or an application processor.

The LED drivers can supply 25 ~ 150 mA current with a 25 mA step to adjust the brightness of the LEDs. Also, the drivers were designed to endure up to 5V of power supply in the event that some LEDs required more than 3V of forward voltage for activation (turning on).

C. BIA AFE

The BIA AFE is comprised of two tetrapolar measurement circuits for full body composition measurement with different excitation frequencies. The BIA AFE with the digital I/Q demodulator obtains the body impedance with substantially low power consumption.

The portion of the circuit consisting of NCO, DAC, OP2, and the optional band-pass filter, shown in Fig.1, applies the AC current, $I(t)$, into the body. Then, $I(t)$ and the voltage drop across the input electrodes, $v(t)$, appears as

$$I(t) = A \sin(\omega_0) \quad (4)$$

$$v(t) = A|Z| \sin(\omega_0 + \theta) \quad (5)$$

Where, Z is the impedance at ω_0 and θ is the phase of the impedance at ω_0 . The digital I/Q demodulator converts the $v(t)$ signal into two DC values, which correspond to the impedance and phase.

The NCO multiplies the digitized signal by $\sin \theta$ and $\cos \theta$ to create an in-phase signal, I , and the quadrature signal, Q . Also, the NCO generates the same clock to drive DAC with the same phase and frequency of $I(t)$. Notably, since the bit resolution of the DAC is 8 bit, the NCO output for the DAC is also represented with 8 bit sign magnitude, whereas the NCO output for the mixers are in 16 bit two's complement. The decimators in I and Q channels produce the DC values as shown in (6) and (7), respectively.

$$I_{DC} = \frac{2A|Z|}{\pi} \cos \theta \quad (6)$$

$$Q_{DC} = \frac{2A|Z|}{\pi} \sin \theta \quad (7)$$

Therefore, the impedance Z can be expressed with θ and $|Z|$ as follows in (8).

$$|Z| = \frac{\pi}{2A} \sqrt{I_{DC}^2 + Q_{DC}^2} \quad (8)$$

The maximum frequency of interest for BIA was set to 1 MHz. Owing to the limitations of single frequency impedance analyzers (e.g. 50 KHz) where current flows primarily through extracellular fluids affording narrow impedance spectrum information, we opted to employ multi-frequency BIA [10]. In the latter system, current penetrates all body tissues thereby permitting a differentiation of total and extracellular fluid compartments in the body. This has further implications for an enhanced estimation of the intracellular water and fat free mass in individuals [10, 11]. Factors that are likely to improve body composition prediction at frequencies ≥ 100 KHz are reduced skin impedance and increased penetration of cell walls.

III. RESULTS

The multimodal sensor AFE IC was designed with 65nm CMOS fabrication technology from Global Foundries (Santa

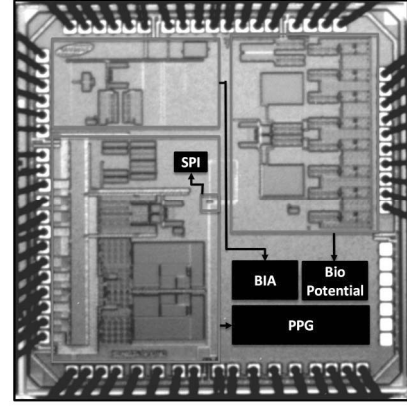


Fig. 3. Photo of the sensor AFE IC.

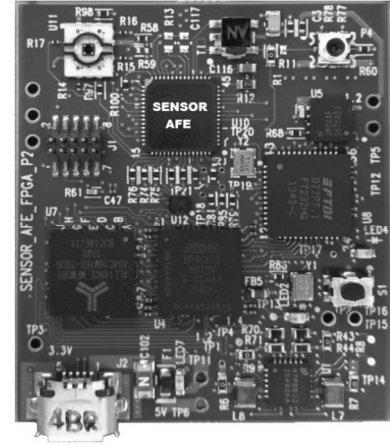


Fig. 2. Sensor AFE evaluation test board.

Clara, CA, USA) via the MOSIS MPW fabrication service. As shown in Fig. 2, the Bio-potential, PPG and BIA AFEs are integrated in the same die occupying $2.5 \times 2.5 \text{ mm}^2$. The evaluation test board for the AFE was also designed with an FPGA (Cyclone IV, Altera Corp., CA) and peripheral ICs such as crystal oscillator, power supplies, and USB Bridge with an area of $4 \times 4.5 \text{ cm}^2$. As shown in Fig. 3, the board is powered via a USB port from an external PC. The board has the necessary DC-to-DC power converter for operating the FPGA and the sensor AFE. The main function of the FPGA is to control and to acquire the data from the sensor AFE IC. Also, the FPGA communicates with the host PC via the USB Bridge IC for the user interface.

The measured power consumption of the sensor AFE IC is presented in Table 2. The static power consumption for each AFE mode is within 380 μW and the dynamic power consumption varies from 0.82 to 1.25 mW per individual AFE

TABLE 2. POWER CONSUMPTION OF THE MULTIMODAL SENSOR AFE IC

Items	Static Power (μW)	Dynamic Power (mW)
Bio-potential	380	0.94
BIA	370	1.25
PPG	340	0.82
Multi-mode	850	1.92

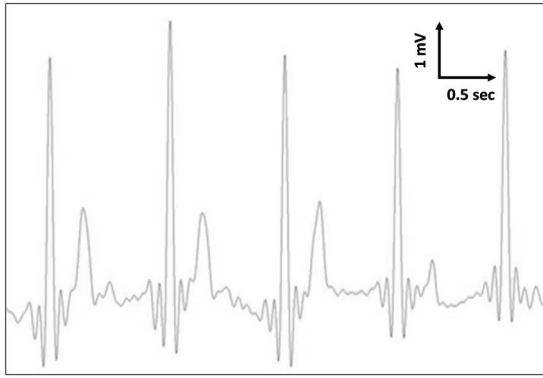


Fig. 4. ECG measurement result from the sensor AFE IC and its evaluation board.

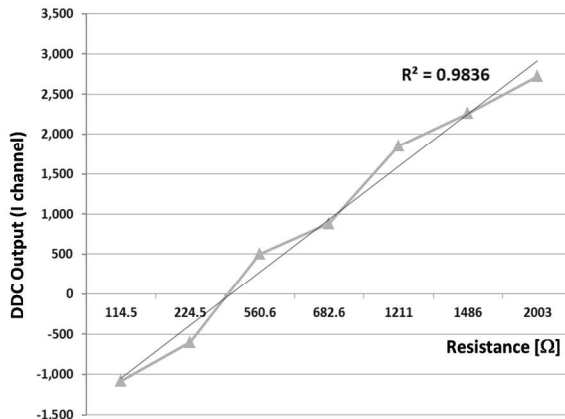


Fig. 5. Measured output of the digital I/Q demodulator (I-channel only) with various resistor values.

operation mode. Notably, these measured values do not include the power consumption of any external components such as LEDs for PPG.

Fig. 4 shows the ECG measurement using the bio-potential AFE designed in this study. For this measurement, two ECG electrodes and a ground electrode were placed on both wrists of a human subject. The sensor AFE IC was operated in the bio-potential mode with a sampling rate of 10 kHz then down-sampled to 500 Hz after the data from the sensor AFE were transferred to the FPGA chip on the evaluation board and subsequently transferred to the PC. For the display purpose the down-sampled data was also high-pass filtered with a cut-off frequency of 0.5 Hz.

To validate the operation of the BIA mode, a resistor of 1 KΩ was connected between a differential input channel in the BIA AFE block, while the stimulation circuitry including the NCO and DAC2 depicted in Fig. 1 applied 100 KHz of sine waves to the resistor. We measured the output of the digital I/Q demodulator using a resistor with various values ranging from 100 to 2.0 kΩ. The actual resistor value was measured by a digital multi-tester to calibrate resistance mismatches between actual and nominal values. The linear regression results show greater than 98% linearity over the resistor value range.

IV. CONCLUSION

The report details the design and development of a multimodal sensor AFE IC with 65 nm CMOS technology. Three sensor AFEs, Bio-potential, PPG and BIA, were integrated on the same die with a modest physical footprint of 2.5 x 2.5 mm². The dynamic power consumption for each AFE mode was within 1.25 mW for all three modes and did not exceed 1.92 mW for the concurrent operation mode, ideally suited for wearable devices.

The novelty of our development lies in its multi-purpose functionality as a non-intrusive wearable device. The platform boasts the advantages of size and low power consumption afforded by implementing common component sharing between all sensing modalities. These types of systems in a wrist watch form factor permit users to self-monitor multiple physiological parameters without the encumbrance of having several body sensors and possessing advanced operational know-how of each modality. Future developments will focus on incorporating refined algorithms and signal processing for extracting several additional parameters such as skin temperature, caloric consumption and blood pressure.

REFERENCES

- [1] A. Pantelopoulou and N.B. Bourbakis, "A Survey on Wearable Sensor-Based Systems for Health Monitoring and Prognosis," IEEE Trans. Systems, Man, and Cybernetics-Part C: applications and Reviews, Vol. 40, No. 1, Jan 2010.
- [2] R. Paradiso, G. Loriga, and N. Taccini, "A wearable health care system based on knitted integrated sensors," IEEE Trans. Information Technology in Biomedicine, Vol. 9, Issue:3, Sep. 2005.
- [3] A. Milenković, C. Otto, and E. Jovanov, "Wireless sensor networks for personal health monitoring: Issues and an implementation," Computer Communications, Vol. 29, Issues 13-14, Aug. 2006.
- [4] H.H. Asada, P. Shaltis, A. Reisner, S. Rhee, and R.C. Hutchinson, "Mobile Monitoring with Wearable Photoplethysmographic Biosensors," IEEE EMBS magazine, May/June 2013.
- [5] Y. Zheng, B. P. Yan, Y. Zhang, and C. Y. Poon, "An Armband Wearable Device for Overnight and Cuff-less Blood Pressure Measurement," IEEE Trans. on Biomedical Engineering, Vol. 61, Issue 7, 2014, pp. 2179-2186.
- [6] P. Giassi, Jr., S. Okida, M. G. Oliveira, and R. Moraes, "Validation of the Inverse Pulse Wave Transit Time Series as Surrogate of Systolic Blood Pressure in MVAR Modeling," IEEE Trans. on Biomedical Engineering, Vol. 60, No. 11, 2013, pp.3176-3184.
- [7] S. Bang, C. Lee, J. Park, and M. Cho, "A Pulse Transit Time Measurement Method Based on Electrocardiography and Bioimpedance," IEEE BioCAS 2009, Beijing, China, Nov. 2009.
- [8] I. Kim, P. Lai, R. Lobo, and B.J. Gluckman, "Challenges in Wearable Personal Health Monitoring Systems," 36th Annual International IEEE EMBS Conference, Aug. 26-30, 2014, Chicago, IL, USA.
- [9] G. Fortino and V. Giampa, "PPG-based methods for non-invasive and continuous blood pressure measurement: an overview and development issues in body sensor networks," 2010 IEEE Int'l Workshop on Medical Measurements and Applications Proceedings (MeMeA), Ottawa, Canada, May 2010.
- [10] W.C. Chumlea and S.S. Guo, "Bioelectrical Impedance and Body Composition: Present Status and Future Directions", Nutrition Reviews, Vol 52, No. 4, 1994.
- [11] Y. Yamada, Y. Watanabe, M. Ikenaga, K. Yokoyama, T. Yoshida, T. Morimoto and M. Kimura, "Comparison of single- or Multifrequency bioelectrical impedance analysis and Spectroscopy for Assessment of Appendicular Skeletal Muscle in the Elderly, J. Appl Physiol., Vol. 115, No. 6, 2013, pp. 812-818.